

Dedicated to Prof. Voicu Lupei's  
70<sup>th</sup> Anniversary

## EDGE-PUMP HIGH POWER MICROCHIP Yb:YAG LASER

TRAIAN DASCALU

National Institute for Laser, Plasma and Radiation Physics,  
Laboratory of Solid-State Quantum Electronics, Bucharest 077125, Romania  
email: traian.dascalu@inflpr.ro, http://ecs.inflpr.ro/

(Received August 12, 2008)

*Abstract.* This paper presents new concepts for pumping very thin active laser media at pump level of hundreds of watts, output performances obtained from Yb-based microchip laser. Continuous-wave (cw) laser operation at 1.03 μm with slope efficiency of 0.40 in Yb:YAG and low thermal lens was realized using an edge-pump configuration and a laser diode emitting at 0.94 μm. Over 90 W cw output power was demonstrated from Yb:YAG volume of  $2 \times 2 \times 0.4$  mm<sup>3</sup>. The optical phase distortion analysis gives focus shift bellow to 0.05 m and proves the absence of astigmatic effects. Two new architectures of thin disc concept were analysed numerically and experimentally. These new design allow very thin disk to be operated at high power level.

*Key words:* lasers and laser optics; lasers, solid-state; lasers, diode-pumped; lasers, ytterbium; thermal effects.

### 1. INTRODUCTION

Power scaling of microchip solid-state lasers is essential for various applications like two-photon microscopy, precise cutting in micromachining, that require a high power, high-quality laser beam from a small dimensions device. The key point in designing a high-power microchip solid-state laser is related to the management of the inevitable generation of waste heat during the pumping process. Typically the diode pumped solid-state lasers have a non-uniform deposition of heat. This fact, combined with the propagation of that heat through the gain medium to the heat sink, results in temperature gradients that turns in gradients in refractive index, thermal lens effects, astigmatic and birefringence effects, and mechanical stress.

The quantum defect of Yb doped laser is typically almost three times lower than that associated with the Nd-doped crystals. However the performance of such a system is intrinsically sensitive to temperature since the thermal population of the lower laser level causes absorption at the laser wavelength.

Appropriate choice of the pump geometry is the key issue in the optimization of diode-pumped ytterbium-doped lasers. A number of representative designs have already been presented in related literature: high-power thin disks with multiple mirrors pumps [1], high-energy cascaded plates [2] with lens-duct coupled large pumps, end-pumped rods [3] and slabs [4], at various pump power levels. One architecture that has been proposed to maximize the benefits of a material like Yb:YAG, whilst minimizing the associated difficulties, is the thin-disk [5, 6] or active mirror [7] laser. Over 1070 W continuous wave (CW) output power with 48% optical efficiency was reported [6]. There are two outstanding advantages of this geometry: large ratio of the cooling surface to the pumped volume and the fact that the direction of heat flow is parallel to the laser cavity axis. This results in purely axial temperature gradients, which in turn implies that the intra-cavity laser field experiences no thermal lens [8].

Perhaps the main disadvantage of the thin-disk laser is the relative complexity of the optical system required to achieve multi-pass pumping and thus efficient absorption. Because the crystal's thickness is several times lower than effective absorption length the unabsorbed pump power is reimaged onto the crystal several times making a complicated setup. Alternative solution is given by edge-pumped [9, 10] composite microchip configuration giving good absorption efficiency while preserves setup's simplicity. Over 90 W output power have been obtained from a CW diode edge-pumped 10 at % Yb:YAG composite microchip of 400  $\mu\text{m}$  thickness [9]. By reducing the crystal thickness to 300  $\mu\text{m}$  over 300 W output power have been reported [11]. The decrease of the crystal thickness to values below 100  $\mu\text{m}$  becomes difficult for edge pumped thin materials because of limited pumping spot size. One configuration that allows the decrease of gain crystal thickness preserving its strength is diffusion bonding of gain media to an index matched undoped cap [12]. The complicated imaging pumping geometry used by thin-disk is replaced by non-imaging lens duct technology. By using re-imaging pumping system a similar arrangement for gain media reported 235 W output power [13], however, nonuniform distribution of the absorbed power was observed in this scheme.

In this work we review three new architectures for a thin-disk laser: all are based on composite structure that consists of thin-disk laser crystal acting as active mirror. The active mirror is bonded to the heat sink by using metallic gold-tin technology:

1. The first architecture is simple edge pumped composite microchip with thickness between 250–400  $\mu\text{m}$ .

2. When the active media thickness is between 100  $\mu\text{m}$  to 250  $\mu\text{m}$  we propose a geometry that consist of small diameter of a thin disc that has on top of it a diffusion bonded undoped material of larger diameter and thickness. The pump beam is delivered through three windows and propagates inside the undoped cap and gain crystal by total internal reflection (TIR). This configuration allows the

multi-pass of the pump beam by using only geometrical design of the composite gain media and keep the pump focusing optics simple and easy to align. The gain media strength is enforced by the undoped cap which provides also the way to concentrate the pump beam uniformly into a small diameter gain media.

3. Composite microchips with thickness lower than 100  $\mu\text{m}$  are not suitable for edge-pumping because it requires complicated optics to focus high power diode lasers bellow this dimension. We want to overcome this impediment by proposing a new design for the geometry of the Yb based microchip laser. It keeps the edge of the crystal large enough for simple diode pumping optics while the doped active region has a thickness bellow 100  $\mu\text{m}$ . The laser gain media has a composite structure that consists of cylindrical core doped gain media (single crystal or ceramic material) surrounded by highly transparent ceramic undoped YAG. A very thin plano-concave lens having all surfaces polished at high quality level is fabricated from the composite material. The diameter of the doped core is around several millimeters.

## 2. RESULTS AND DISCUSSION

### 2.1. LASER HEAD CONFIGURATION FOR EDGE-PUMP COMPOSITE MATERIAL

The composite microchip laser heads we use for high-power generation, in all three models presented below, are produced by using similar technologies. First technology is related to *diffusion bonding*. The composite material consisting of  $2 \times 2 \text{ mm}^2$  Yb:YAG core doped 10 at. % Yb is diffusion bonded to 10 mm diameter undoped YAG clad. The result is a free of defects Yb:YAG/YAG interface with just a very small refractive index difference. The thin slice of Yb:YAG/YAG composite material is polished at laser quality. The back surface is flat and coated for high reflectivity at 1030 nm. The other key technology for high-power microchips is *die-bonding* and it is related to heat removal from microchip volume. The quantum defect of Yb:YAG lasing at 1030 nm is quite small (8.6%) comparative to Nd:YAG but small volume high power laser makes temperature reach over 200°C. Yb:YAG has quasi-three levels and its efficiency is very sensitive to temperature, therefore the design of high-power microchip laser try to minimize the distance the heat has to move toward the cold surface and maximize the cooling system efficiency. The crystal is bonded to highly efficient cooling system by using gold-tin die-bonding technology. The soldering temperature peaks at 280°C therefore all dielectric coatings have to be work proof at this temperature.

Folowing we describe three new laser architectures based on the ideas presented above.

### 2.1.A. Edge pumped microchip

Fig. 1 presents the microchip Yb:YAG/YAG laser under a four-fold diode laser pumping scheme. The composite crystal consists of a Yb:YAG core of square shape that is diffusion bonded to an undoped YAG region. The crystal has one surface high-reflectivity (HR) coated at the laser wavelength of 1030 nm; this side was in contact with a 100 W class microchannel cooling system, while a soldering technique was used to decrease the thermal impedance between these two surfaces. The crystal's opposite side was antireflection coated at the laser wavelength. Four fiber-coupled lasers JOLD-100-CAXF-15A (JenaOptik), each of which delivered 100 W output power at 940 nm were used for edge pumping.

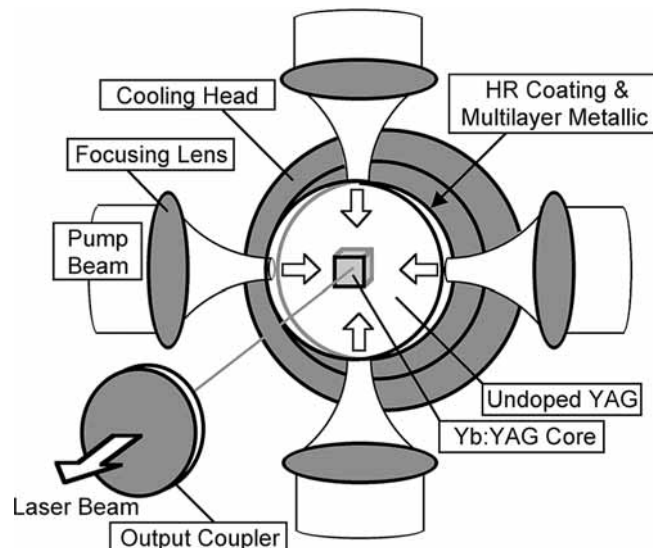


Fig. 1 – Schematic representation of Yb:YAG edge pump microchip laser.

The pump light was inserted into the undoped YAG crystal through four windows of  $400 \mu\text{m} \times 2 \text{ mm}$  dimensions each. In order to avoid the parasitic oscillations the opposite input windows were made inclined (3 to 5 degree) with respect to each other, while the remained cylinder edge was rough polished in order to act as a diffuser. Inside the microchip the pump light propagates by total internal reflection to match perfectly the Yb:YAG core, where it is partially absorbed. The remaining light reaches the edge of the undoped YAG: part of it is lost through the pumping windows, whereas the remaining light is scattered back into the microchip.

### 2.1.B. Top cap thin-disk Yb:YAG/YAG composite microchip laser

Fig. 2 shows a new design for a thin-disk Yb:YAG/YAG composite microchip laser. The thin Yb:YAG gain media with diameter  $\phi$  and thickness  $t_2$  is

diffusion bonded to an undoped YAG cap of diameter  $\Phi$  and thickness  $t_1$ . Three pump windows spaced at  $120^\circ$  each one and  $45^\circ$  with respect to the optical axis were cut on the undoped YAG cap. The pump beam impinges perpendicular onto window surface and propagates by TIR between the top and bottom surfaces of the microchip as shown in Fig. 2a. Let us consider a ray that propagates from the pump window and makes an angle  $\gamma$  with the corresponding radius (Fig. 2b).

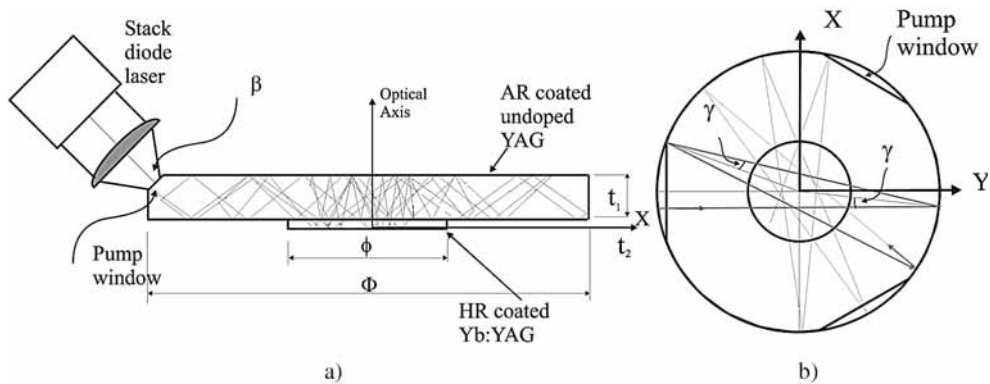


Fig. 2 – Ray tracing through composite microchip: a) side view; b) top view.

The undoped YAG cap allows the transverse pump to multi-pass forth and back the gain medium through TIR analogous to the pumping method in a doubly clad fiber laser. When the pump light intersects the gain media it is partially absorbed, then it is reflected and propagates towards cylindrical surface of the undoped YAG. After TIR on this surface the ray and the reflection plane make the same angle  $\gamma$  with respect to the radius. Therefore the ray hits again the gain media

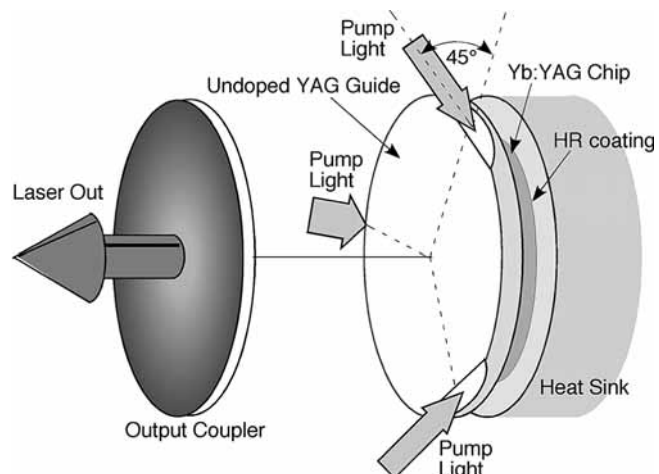


Fig. 3 – Schematic view of cap thin-disk Yb:YAG/YAG composite microchip laser.

and the process continues until it is entirely absorbed, or eventually escapes through one of the three pump windows. The maximum pump beam divergence that still propagates through the YAG cap by TIR is  $43.2^\circ$ . The Yb:YAG chip has its bottom surface high-reflection (HR) coated at the lasing wavelength of 1030 nm and HR coated at 940 nm for  $38^\circ$  to  $52^\circ$  angles of incidence.

A metallic coating can be finally used in order to solder the Yb:YAG/YAG to a cooling finger and to obtain an efficient heat transfer between them, as presented in Fig. 3.

### 2.1.C. Lens Chip Active Media

The structure proposed to be analysed is a composite one that consists of cylindrical core doped gain media (single crystal or ceramic material) surrounded by highly transparent ceramic undoped YAG. The fabrication process is specific to ceramic technology not to diffusion bonding. A very thin plano-concave lens having all surfaces polished at high quality level is fabricated from the composite material.

The flat surface of the microchip has high reflectivity dielectric coating and is attached to a heat sink by using gold-tin technology in order to have an efficient heat transfer, Fig. 4. The design makes use of several collimated high power naked diode lasers surrounding, in a circular arrangement, the laser gain media. By using a cylindrical lens the pump radiation is focused on the microchip's edge and propagates by total internal reflection (TIR) inside the gain media. Because of the lens shape design the pump beam changes its direction many times inside the core giving good absorption efficiency. Depending on the doping level and on the core's diameter, good absorption uniformity may be obtained. The important advantage of

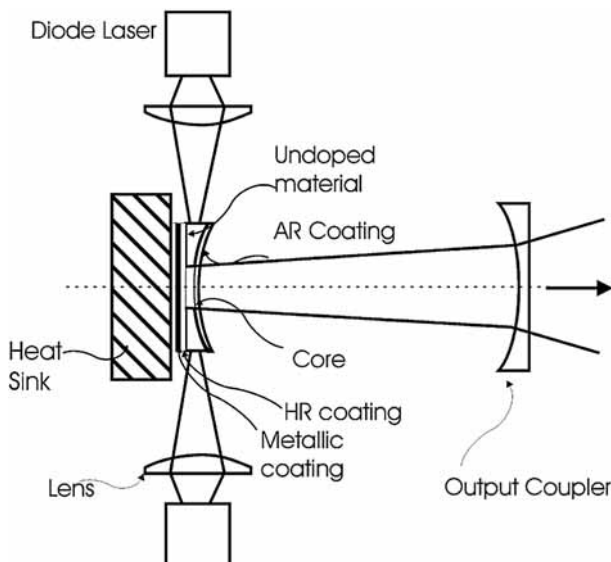


Fig. 4 – Edge pumped lens-shape gain media laser, side view.

this configuration is given by the very thin-disk laser crystal working as an active mirror which allows high power laser operation while keeping the temperature at low level. This arrangement is very attractive especially for quasi-three level lasers like Yb:YAG or Yb:KGW which are sensitive to the operation temperature.

## 2.2. NUMERICAL SIMULATIONS

There are several parameters which have to be taken into account when designing high power lasers. They are related to optical and spectroscopic characteristics of the active media, thermo-mechanical parameters, heat flow in solids, etc. Some of them are well known (lifetime, emission and absorption cross sections, doping level, fracture limit, quantum efficiency, etc.) others (thermal impedance, heat conductivity, etc.) need to be carefully measured. There are three important kind of numerical simulations we performed in order to predict the results for microchip laser. First, the absorption efficiency and absorbed power distribution inside the doped crystal are calculated. In order to do it we use ray tracing software RAYICA adapted to our geometrical configuration. The diode laser pump beam was simulated as close as possible to that of JOLD-100-CAXF-15A (JenaOptik) diode laser for the architecture A and B and for architecture C we use diode laser JOLD 940 QAFN 6A. Secondary, we used the absorbed power distribution to calculate by finite element analysis (FEA) the temperature and stress fields inside crystal. Finally, the information from temperature, absorption and stress are combined with those related to laser resonator and give the predicted power threshold, slope efficiency and output power.

### 2.2.A. Numerical simulations of edge-pump thin-disk Yb:YAG/YAG

The results obtained from numerical simulation of pump beam absorption in edge-pump configuration are presented in Fig. 5a and compared with the experimental fluorescence image, Fig. 5b. The crystal thickness is 400  $\mu\text{m}$ , square core of  $2 \times 2 \text{ mm}$ , 10 at % Yb doping level and it is pumped by four diode lasers optical fiber delivery, 100 W each, 940 nm wavelength. The fluorescence image is taken by CCD camera close to the Yb:YAG core. The pump beam absorption efficiency was evaluated as 74%, in very good agreement with the experimental value. Thus, this pumping geometry eliminates the rather complicated optics used in the disk laser geometry, but still assure a high value for the pump's beam absorption efficiency.

The numerical result of absorbed power distribution is then used for FEA in order to find out the temperature field and mechanical stress inside the thin crystal. Fig. 6 shows that the heat flows almost axially and low thermal distortion of the laser beam is expected. This fact was proven experimentally by phase distortion experiment, see Section 2.3.A. The maximum temperature of the upper surface of Yb:YAG crystal was 220°C when pump power is 400 W.

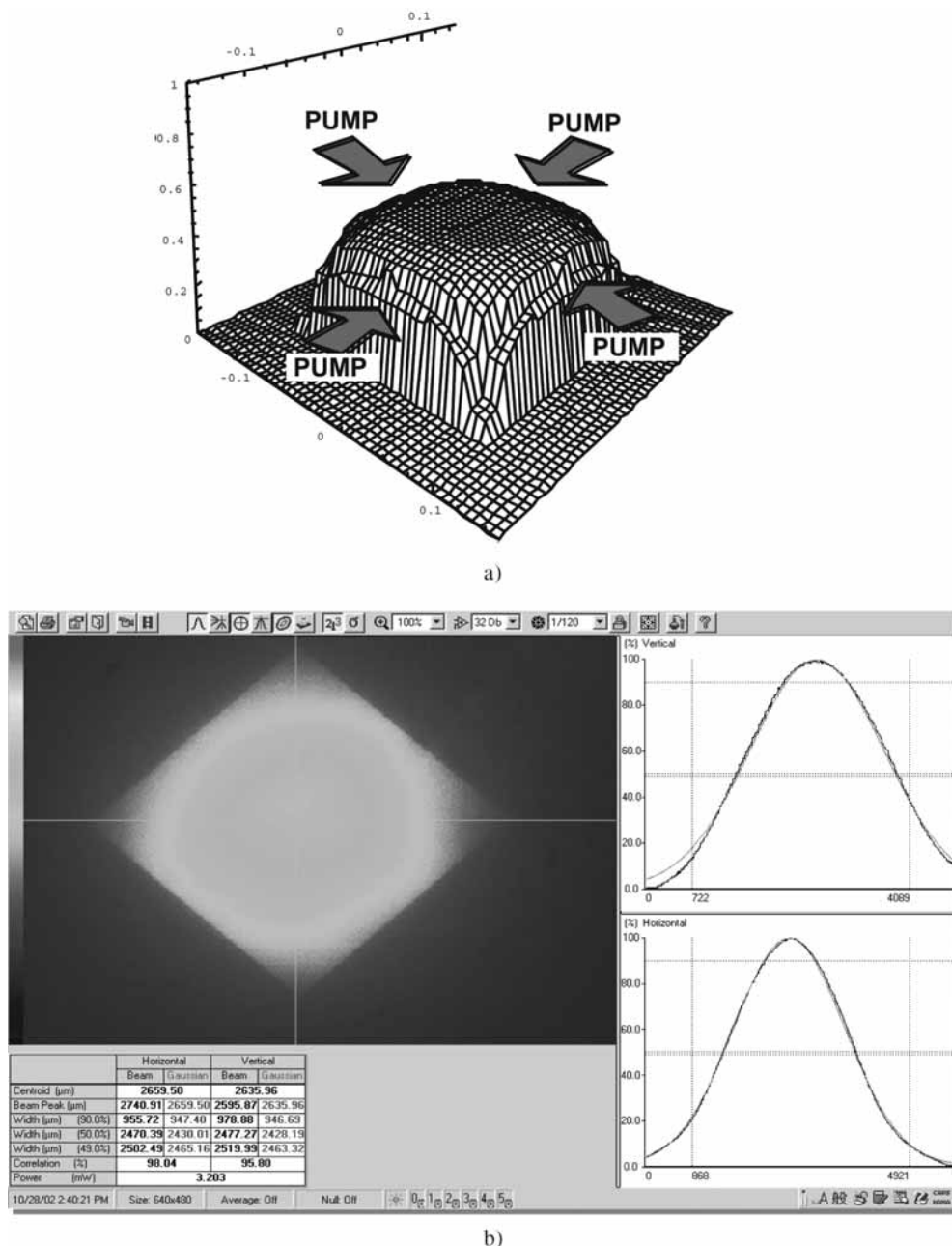


Fig. 5 – a) Distribution of fluorescence intensity in  $2 \times 2$  mm Yb:YAG core under four directions pumping obtained by ray tracing method; b) experimental pump-beam distribution (fluorescence image taken by CCD camera).

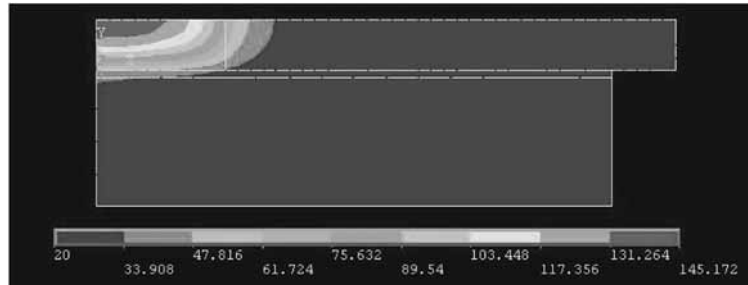


Fig. 6 – Temperature distribution calculated by finite element method, (ANSYS software) for microchip of 400  $\mu\text{m}$  thickness,  $2 \times 2 \text{ mm}^2$  Yb:YAG core, gold-tin metallic bonding to Cu-W heat sink.

## 2.2.B. Numerical simulations of top cap thin-disk Yb:YAG/YAG

The pump beam distribution at each window was recorded with a CCD camera and used in simulations on the absorption efficiency and pump beam distribution into the Yb:YAG crystal.

We further comment that because of Yb:YAG thickness,  $t_2$ , each time when the ray crosses the gain media a small displacement  $2t_2 \times \tan[\pi/4 - \arcsin(\sin\beta)]$  is added in the XY plane,  $\beta$  is the incident angle as shown in Fig. 1b. Thus, the non uniformities reported in Ref. [13] are eliminated because of a multi-pass absorption with different ray orientation instead of one pass absorption and due to the optical path added to the ray path each time when the ray strikes the gain media.

The pump-beam absorption efficiency and its distribution into the Yb-doped medium were numerically evaluated by RAYICA ray tracing software and the Monte Carlo method. The dependence of the absorption efficiency on geometrical and material factors was analyzed. Fig. 7(a) shows the numerical simulation of absorbed power distribution for three pumping directions and Fig. 7(b) shows the experimental fluorescence image of the pumped Yb:YAG core. The agreement between simulations and experiment is very good taking into account the fabrication differences of diode lasers.

The pump absorption uniformity is important for keeping pure axial thermal gradients into Yb:YAG gain media that makes possible the generation of laser beam with high quality. In order to characterize the distribution of the absorbed pump power into the gain medium, we defined a normalized uniformity as  $U = [\langle I \rangle - \sigma_I]/\langle I \rangle$ , where  $\langle I \rangle$  is the average value of the irradiance absorption inside of the gain media and  $\sigma_I$  is the variance inside the gain media volume integrated over the optical axis. Following this definition, the optimum pump absorption distribution has  $U$  coefficient close to one. The uniformity coefficient varies periodically with cap diameter as Fig. 8(a) shows. Because the absorption efficiency,  $\eta_a$  depends on the product of absorption length and absorption coefficient

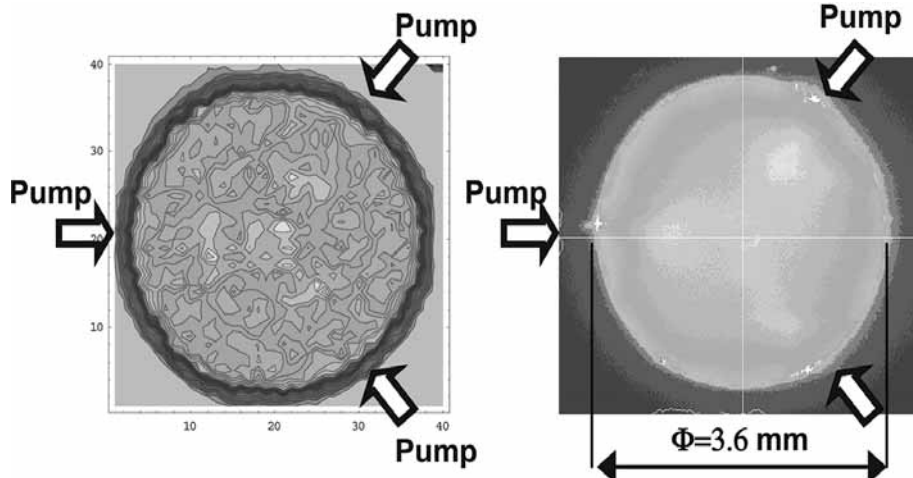


Fig. 7 – a) Ray tracing numerical simulation of pump beam absorption distribution, lines show equal intensity contours; b) the fluorescence image of Yb:YAG core, under pumping by three diodes with  $0.39 \text{ mm} \times 3.6 \text{ mm}$  pump spot size.

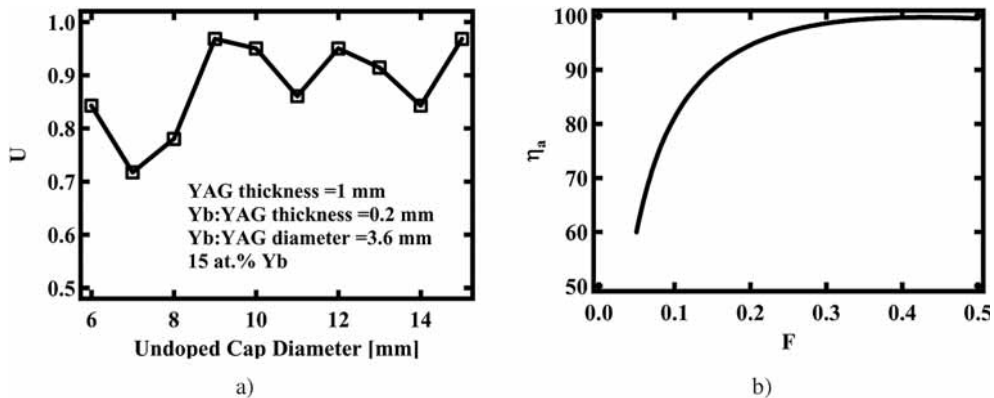


Fig. 8 – a) Uniformity factor vs. undoped cap diameter; b) absorption efficiency vs.  $F$ .

in our case a good figure of merit for  $\eta_a$  is  $F = t_2 \times \alpha_a$ , with  $\alpha_a$  the absorption coefficient. Figure of merit larger than 0.15 yields over 90% absorption efficiency (Fig. 8b). Proper choice of geometrical parameters as well as doping level is important for obtaining, from the same microchip, good  $U$  and high  $\eta_a$ . For example a configuration that has the gain media of 25 at % Yb:YAG of 75  $\mu\text{m}$  thickness gives more than 90 % absorption efficiency [14]. High absorption efficiency can be obtained by decreasing the cap thickness  $t_1$  and by increasing the doping level and Yb:YAG thickness  $t_2$ , however this comes at the expense of a low homogeneity of the absorbed pump power distribution in the Yb:YAG crystal.

It can be seen from Fig. 9a that there is an optimum value for cap diameter. Small cap diameter gives low absorption efficiency because the ratio between pump window surface and cap surface is large therefore there is high probability for ray to escape. Very large cap diameter implies many TIRs therefore the probability for scattering by surface defects increases and the losses increase too. The absorption efficiency increases slightly when cap thickness decreases. It is possible to obtain 95% absorption efficiency with uniformity factor of 0.95 [14].

The temperature distribution into Yb:YAG gain media can be calculated following the method proposed by Cousins [15]. Whilst the analytical modeling is very good for identifying the important parameters, the complexity of the structure shown in Fig. 3 requires the use of FEA. The temperature distribution in Yb:YAG/YAG structure generated by the absorbed power was calculated by using the finite element software, ANSYS 7.0.

Fig. 9a shows the temperature of the upper YAG's cap surface *versus* pump power when thermal conductivity of the heat sink's material is copper-tungsten (Cu30-W70,  $K = 180 \text{ Wm}^{-1}\text{K}^{-1}$ ) and diamond like material (DMCH60,  $K = 550 \text{ Wm}^{-1}\text{K}^{-1}$ ). We neglect in this case the thermal impedance introduced by HR dielectric layer and suppose very thin Au-Sn die bonding layer. Fig. 9b shows the temperature of the YAG upper surface *versus* pump power when Yb:YAG thickness varies from 200  $\mu\text{m}$  to 50  $\mu\text{m}$ .

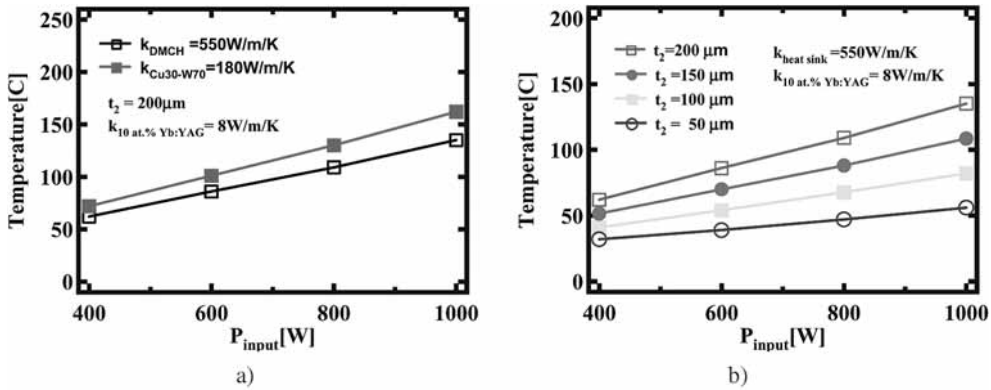


Fig. 9 – a) The FEA calculated temperature of the Yb:YAG upper surface *vs.* the pump power for two different heat sinks materials; b) the FEA calculated temperature of the Yb:YAG upper surface *vs.* the pump power for different Yb:YAG thicknesses.

Comparing these two figures it comes out that the Yb:YAG thickness reduction has a much more influence on temperature than the increased thermal conductivity of the heat sink. Increasing the heat sink thermal conductivity from  $180 \text{ Wm}^{-1}\text{K}^{-1}$  to  $550 \text{ Wm}^{-1}\text{K}^{-1}$  makes the temperature decrease by 20% while the decrease of gain media thickness from 200  $\mu\text{m}$  to 50  $\mu\text{m}$  makes temperature decrease from 140°C to 50°C even if the absorbed pump density increases four

times. We found that the design of a thin Yb:YAG gain media assembled with undoped YAG develops a thermal gradient very close to that of a cap-less thin-disk. Thus, this composite structure maintains the thermal advantages of a thin-disk geometry, while enabling high pump power to be easily injected through the pump windows, trapping it within and hence multi-passing forth and back the gain media. The cap simply rises to a uniform, constant temperature, a harmless effect that does not affect the thermal gradients in the thin gain media.

Similar computations were made for different values of crystal to heat sink thermal impedance, see Ref. 14.

### 2.2.C. Numerical calculations of Lens Chip active media

Fig. 10 shows ray tracing simulation obtained by using the RAYICA software. The pump beam parameters used in these simulations are those of high power six stack diode laser, 10 mm wide, 1.75 mm pitch, 34° fast axis divergence and 6° slow axis divergence.



Fig. 10 – Yb:YAG/YAG microchip laser: side view of the ray propagation inside of the microchip (ray hits first the spherical surface).

A numerical model is used for design and operation parameters of lens shape microchip laser that is expected to work at higher temperature. In particular, it allows the determination of the scaling properties of this laser concept. As the temperature distribution inside the crystal has a strong effect on the output power, a detailed knowledge of the heat conductivity is important. We use the data provided by Ref. 6. The generation of the heat is assumed to result from the Stokes defect of 8.6% between the energy of the pump and the laser photon. The heat load is calculated according to the distribution of the absorbed pump radiation. In the calculations a heat resistance between the crystal and the cooling medium is included, which is determined from finite-element calculations taking into account the cooling medium.

For the pump configuration mentioned above optical efficiencies as shown in Fig. 11a and 11b are calculated versus pump power. The parameters are total loss  $\gamma$  and ratio of total loss and reabsorption loss,  $B$ . Optical efficiency is defined here as the ratio between laser output power and pump radiation power entering the pump optics. With 1000W pump power the output power is 480W with 92% absorption efficiency and 52% slope efficiency and a maximum temperature of the crystal at the front side of 160°C. With higher pump power, the absorption efficiency is reduced due to higher temperature (quasi-four level laser condition) and ground state depletion. The optical efficiency can be raised by reducing the heat resistance

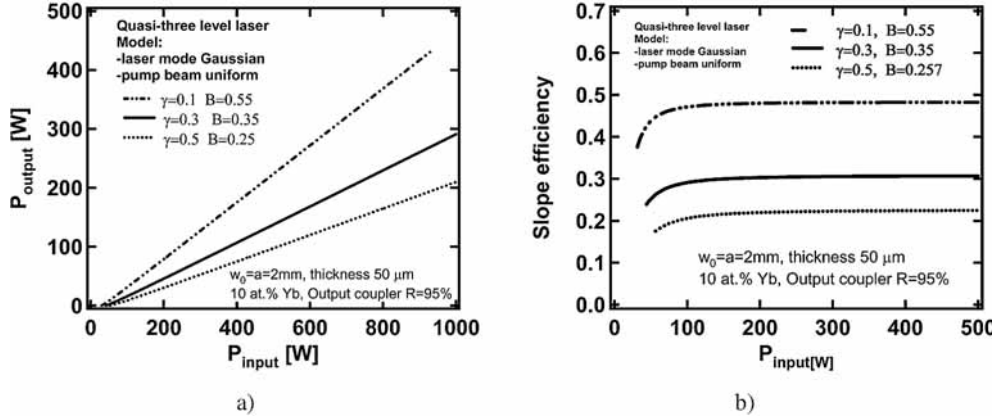


Fig. 11 – a) Output power *versus* input power for quasi-three level laser; b) slope efficiency *versus* input power power for quasi-three level laser.

between crystal and cooling fluid. A thermal resistance reduction of  $2\text{ Km}^2/\text{W}^{-1}$  increases optical efficiency by 2%. The optical efficiency increases by doping level increase. In case of thin disk operation where absorption depends on the thickness of the crystal there is an optimal thickness which maximize the absorption and minimize reabsorption losses [16]. The microchip lens shape active media do not show such optimal thickness because the absorption efficiency depends on the diameter of the doped core not by its thickness. Therefore lower the thickness lower the temperature of the front side of the crystal and lower the re-absorption losses. However there is an optimal doping level in order to keep an uniform absorption over the core area. Numerical simulations with ray tracing software have shown that around 3 at % doping level is optimal for obtaining 0.90 uniformity as defined in Ref. 14 for 4 mm core diameter and seven diode laser pumping simmetrically distributed around lens chip.

The temperature distribution in a lens-shape active laser media was calculated by FEA, the temperature of the front surface decreases 2 times when the thickness is reduced from  $200\mu\text{m}$  to  $50\mu\text{m}$ , even if the pump power absorption density is increased **four times**. Detailed analysis of lens-shape microchip is given in Ref. 17.

## 2.3. EXPERIMENTAL RESULTS

### 2.3.A. Experimental result for edge-pump thin-disc laser

Fig. 12 presents the cw output power of the microchip Yb:YAG laser function of pump power. A plane-concave resonator of 50 mm length with an output mirror of 100 mm radius and transmission ( $T$ ) between 3 and 10% was used in experiments. A maximum power of 90.2 W for a 340 W pump power was obtained for the mirror with  $T = 5\%$ ; the threshold of laser operation was  $\sim 55\text{ W}$

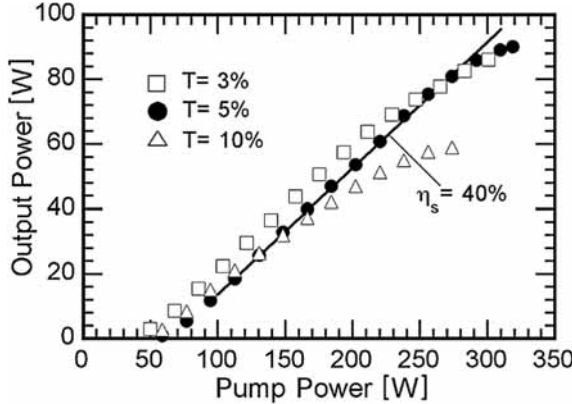


Fig. 12 – Cw output power *versus* pump power for the radial pumped microchip composite Yb:YAG/YAG laser.

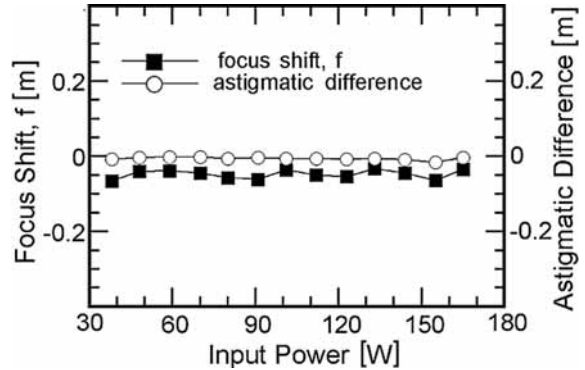
and the slope efficiency evaluated at pump power at least two times larger than the threshold was 40%. For the  $T = 3\%$  output mirror the threshold decreases at  $\sim 40$  W but the slope efficiency decreases at 37%, while the lower slope efficiency of 31% was obtained for the mirror with  $T = 10\%$ . For the maximum pump power the laser beam was highly multimode, very close to top hat like distribution. In order to improve the laser beam transverse distribution a V-type resonator, consisting of a plane-concave (1 m radius output mirror) resonator of 660 mm length with the medium placed 360 mm apart of the plane HR rear mirror, was build. With an output mirror of  $T = 5\%$  the output power decreased by  $\sim 25\%$  compared to the linear resonator, but the laser beam  $M^2$  factor was kept almost constant,  $\sim 5$ , over the entire pumping range. Because in the V-type resonator the laser beam filled the Yb:YAG core, the power decrease was mainly attributed to some additional diffraction losses that could occurs on the bonded interfaces of the composite medium.

It is worthwhile to mention that when the Yb:YAG/YAG laser was quasi-cw pumped (10 Hz repetition rate, 10% duty factor) the maximum output power obtained for the linear resonator with the  $T = 5\%$  output mirror was 135 W (40% optical-to-optical efficiency) with 40% slope efficiency. Because of some limitations, the cooling water temperature could not be reduced under 15°C during these experiments. Therefore, the slowing down of the slopes efficiency for the cw operation beyond pump power in excess of  $\sim 300$  W was attributed to the thermal dependant reabsorption losses and inefficient laser extraction.

The optical phase distortions induced by the pumped microchip Yb:YAG/YAG on the laser beam were next determined by using a Wavefront Analyser CLAS 2D (WaveFront Sciences Inc.) in the setup presented in Ref. 10. Fig. 13 presents the focus shift  $f$  and the astigmatic difference function of the input power.

The obtained values are almost constant, 0.05 m focus shift and 0.01 m astigmatic difference, for a pump power range from 40 W to up to 180 W proving the axial heat flow and symmetrical absorption in Yb:YAG core. Thus, the wavefront

Fig. 13 – Focus shift and astigmatic difference between sagittal and tangential plane in the microchip Yb:YAG composite laser.



distortions consist only of lensing, free from astigmatism or spherical aberration, which proves the absence of detrimental effects such as stress-induced birefringence.

### 2.3.B. Experimental results of top cap thin-disk Yb:YAG/YAG laser

In experiments we considered a 200  $\mu\text{m}$  thick, 15 at % Yb:YAG gain crystal of 3.6 mm diameter that was attached by diffusion bonding to an undoped 1.0 mm thick YAG of 10 mm diameter (as shown in Fig. 2). Three windows, spaced at 120° each one, were cut at 45° on the YAG component. The window's dimensions are 3.6 mm length and 0.4 mm width. The upper side of YAG crystal was AR coated at the 1030 nm lasing wavelength. The bottom side of Yb:YAG crystal was HR coated at 1030 nm and at 940 nm in such a way that it assures protection against evanescent wave and TIR for pump beam. Because of laboratory conditions the Yb:YAG/YAG structure was attached to a micro-channel cooling system by using a thermo-conductive paste (thermal conductivity  $K = 0.84 \text{ W m}^{-1} \text{ K}^{-1}$ ).

We use for pump three fiber-coupled diode lasers JOLD-100-CAXF-15A (JenaOptik), each of it delivering 100 W at 940 nm ( $\Delta\lambda \sim 4.0 \text{ nm}$ , FWHM definition) through a fiber of 600  $\mu\text{m}$  core diameter and 0.22 numerical aperture. A set of cylindrical and spherical lens was used to image the optical fiber's end onto the pump window. Two different pump spot sizes were used in our experiments: one that has 0.4 mm  $\times$  0.93 mm and does not fill completely the gain media, the second has 0.39 mm  $\times$  3.6 mm and fill the gain media entirely.

The output power versus input pump power performances of this new geometry was investigated in a short plane-concave resonator, as shown in Fig. 3. The thermo-conductive paste, that we used for heat sink contacting, do not allow high-power CW operation, however it is possible to test the laser oscillation under quasi-CW operation. Fig. 14 presents the output power under quasi-CW pumping with 10 ms pulse duration and 5% duty cycle. The best results were obtained in a 50 mm long resonator with a 100 mm radius output mirror of  $T = 0.05$  transmission at 1030 nm: the on-time output power was 34 W for an on-time pumping power of

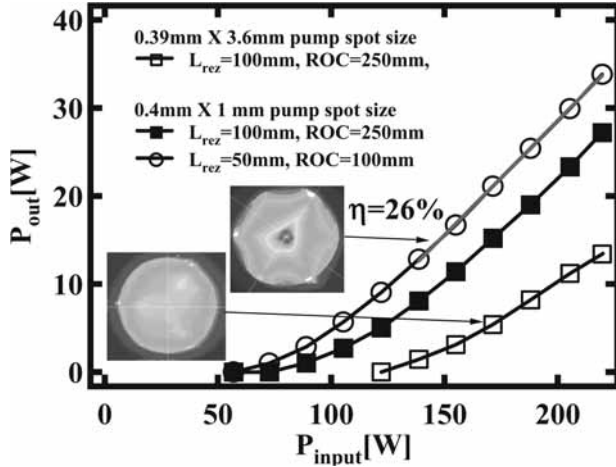


Fig. 14 – On-time output power obtained from the 15 at % Yb:YAG / YAG laser under pumping with three fiber-coupled diode lasers.

220 W with 0.26 slope efficiency. Under pumping with extended pump spot size the fluorescence image of the pumped gain media shows uniform fluorescence emission while under pumping with small pump spot size the fluorescence image shows higher intensity at the center, as shown in the inset of Fig. 14.

Because three pump beams with 0.4 mm × 1 mm pump spot size give higher absorption at the gain media center the pump intensity at center overcomes in higher proportion the laser oscillation threshold giving better slope efficiency. Thus, the pump intensity is only 1.3 times higher than pump intensity at threshold: one could expect a significantly improved slope efficiency if the pump intensity exceeds threshold intensity by more than eight times. In addition, these results are severely impeded by optical fiber delivery diode laser used. The rectangular shape required for efficient coupling the pump beam to gain media is much easier to obtain from a stack diode laser. Moreover, for these preliminary experiments we used thermo-conductive paste therefore the heat transfer was not good enough for high power operation: a metallic coating would be the most appropriate and considered in further work. The laser results are below expectations, but encouraging for the experimental conditions we used. Thus, we consider that by solving these problems, CW operation of 300 W output power with over 40% slope efficiency is possible.

### 3. CONCLUSIONS

In conclusions, we have reported on three new architectures of composite Yb:YAG/YAG microchips. First, cw operation with 90 W output power from a simple edge-pumped composite microchip Yb:YAG/YAG laser was reported. Measurements of the optical phase distortions induced by pumping gives focus

shift below 0.05 m and shows the absence of astigmatic effects, indicating the axial heat flow in this pumping configuration. The output power of microchip composite laser can be further scaled by increasing the Yb:doped core diameter keeping constant the pump power density and by decreasing the crystal's thickness.

Secondary, a new design for microchip laser that allows a reduced thickness of the gain media while keeping the pump optics simple and preserve high absorption efficiency, good thermal management, and uniform pump-beam absorption was demonstrated. The configuration consists of a thin-disk Yb:YAG gain medium that is diffusion bonded to an undoped YAG of bigger diameter, the last acting as a guide for the pumping light. The cap allows pump beam multi-pass the gain media and gives the flexibility to choose the proper gain media diameter for specific applications. Numerical model shows the dependencies between cap thickness and diameter, dopant concentration and gain media thickness. It is shown that there is an optimum cap diameter and the uniformity parameter varies periodically with the cap diameter. Also, it is concluded that for the absorption efficiency over 90% the product of gain media thickness and absorption coefficient should be over 0.15. First experiments yielded on-time 34 W output power for an on-time pump power of 220 W with 0.26 slope efficiency and shows a very homogeneous pump beam. Further work plans using high-power stack diode laser and die-bonding Au-Sn technology for high-power cw operation. The device has large capability for power scaling since available input power is not dependant by gain media thickness like edge-pumping scheme and the undoped YAG cap provides multi-pass efficient absorption. Third: A promising alternative for edge pumped composite microchip laser is presented. The proposed design combine the simplicity of edge-pumping with the effectiveness of active mirror cooling for very thin active laser material. The analysis of the thermal gradients by using finite element method proved the axial heat flow therefore the output power can be truly scaled up without adverse effects on thermal lens. Over 400W output power is predicted with more than 52% slope efficiency.

*Acknowledgments.* The author thanks to Prof. Dr. Voicu Lupei, for the support, guidance, help and suggestions during long period of working together in Laboratory of Solid-State Quantum Electronics. T. Dascalu acknowledges research collaboration between the Laser Research Center of Institute for Molecular Science, Okazaki, Japan, Fukui Industrial Support Center, Japan and Laboratory of Solid-State Quantum Electronics. The Romanian Ministry of Science and Research supported partially this work through the CEEX D07-27 project.

## REFERENCES

1. K. Naito, M. Yamaoka, M. Nakatsuka, T. Kanabe, K. Mima, C. Yamanaka, S. Nakai, *Conceptual Design Studies of a Laser Diode Pumped Solid State Laser System for the Laser Fusion Reactor Driver*, Jpn. J. Appl. Phys. Part 1, **31**, 259–273 (1992).
2. A. Giesen, H. Hugel, A. Voss, K. Wittig, U. Brauch, H. Opower, *Scalable concept for diode-pumped high-power solid-state lasers*, Appl. Phys., B **58**, 365–372 (1994).

3. E. C. Honea, R. J. Beach, S. C. Mitchell, J. A. Skidmore, S. A. Payne, P. V. Avizonis, *High-power dual-rod Yb : YAG laser*, Optics Lett., **25**, 805 (2000).
4. T. S. Rutherford, W. M. Tulloch, S. Sinha, R. L. Byer, *Yb:YAG and Nd:YAG edge-pumped slab lasers*, Opt. Lett., **26**, 986 (2001).
5. A. Giesen, H. Hugel, A. Voss, K. Wittig, U. Brauch, H. Opower, *Scalable concept for diode-pumped high-power solid-state lasers*, Applied Physics B: Lasers and Optics, **58**, 365–372 (1994).
6. C. Stewen, K. Contag, M. Larionov, A. Giesen, H. Hugel, *A 1 kW CW thin disc laser*, IEEE J. Sel. Top. Quantum Electron., **6**, 650–657 (2000).
7. D. C. Brown, R. Bowman, J. Kuper, K. K. Lee, J. Menders, *High average power active-mirror amplifier*, Appl. Opt., **25**, 612–618 (1986).
8. T. Dascalu, T. Taira, N. Pavel, *Thermo-optical effects in high-power diode edge-pumped microchip composite Yb:YAG laser*, Conference Digest of CLEO/QELS Europe 2003, CA8-3, Munchen, Germany, June 22–27, 2003.
9. T. Dascalu, T. Taira, N. Pavel, *100W quasi-continuous-wave diode radially pumped microchip composite Yb:YAG laser*, Opt. Lett., **27**, 1791 (2002).
10. T. Dascalu, N. Pavel, T. Taira, *90 W continuous-wave diode edge-pumped microchip composite Yb:Y<sub>3</sub>Al<sub>5</sub>O<sub>12</sub> laser*, Appl. Phys. Lett., **83**, 20, pp. 4086–4088 (2003).
11. M. Tsunekane, T. Dascalu, T. Taira, *High-power diode-edge pumped single-crystal Yb:YAG/ceramic YAG composite microchip Yb:YAG laser for material processing*, Conference Digest of CLEO/QELS 2005, CTuZ3, Baltimore, Maryland, USA, May 22–27, 2005.
12. L. E. Zapata, S. M. Massey, R. J. Beach, S. A. Payne, *High average power Yb:YAG laser*, presented at Solid State and Diode Laser Technology Review, Albuquerque, New Mexico, USA, May 21–25, 2001.
13. S. Yamamoto, T. Yanagisawa, Y. Hirano, *High power continuous-wave operation of side-pumped Yb:YAG thin disk laser*, Conference Digest of CLEO/QELS 2004, CWO3, San Francisco, CA, USA, May 16–21, 2004.
14. T. Dascalu, T. Taira, *Highly efficient pumping configuration for microchip solid-state laser*, Optics Express, **14**, 670 (2006).
15. A. Cousins, *Temperature and thermal stress scaling in finite-length end-pumped laser rods*, IEEE J. Quantum Electron., **28**, 1057–1069 (1992).
16. D. Kouznetsov, J. F. Bisson, K. Takaichi, K. Ueda, *High-power single-mode solid-state laser with a short, wide unstable cavity*, J. Opt. Soc. Am., B **22**, 1605 (2005).
17. T. Dascalu, C. Dascalu, *High-power lens-shape diode edge-pumped composite laser*, Proc. SPIE, Vol. **6785**, 67850B (2007).